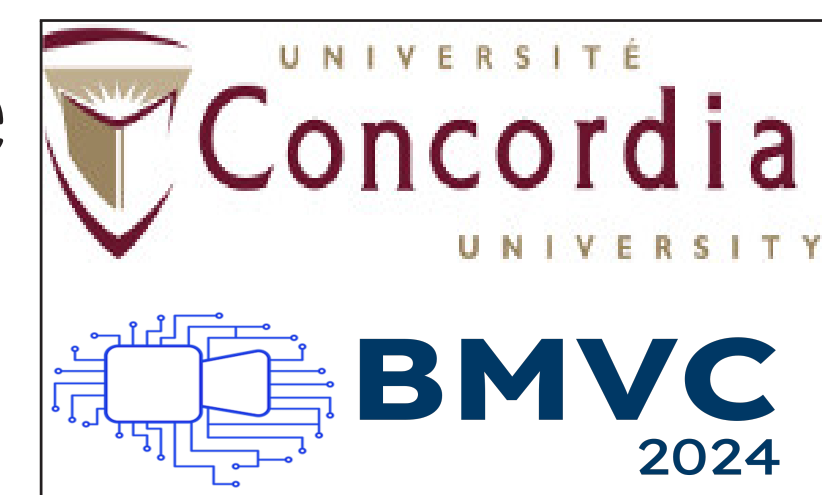


Flexible Graph Convolutional Network for 3D Human Pose Estimation

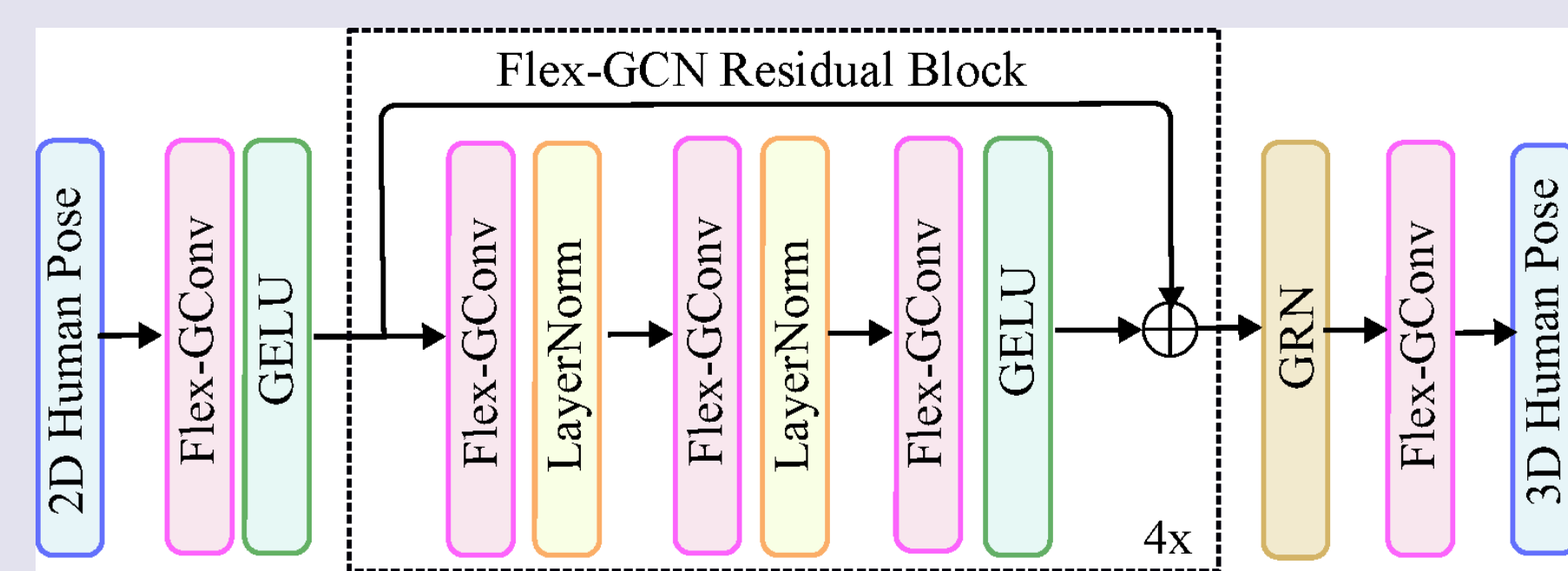
Authors : Abu Taib Mohammed Shahjahan and A. Ben Hamza



Contributions

- Present a flexible graph convolutional network (Flex-GCN), which captures highorder dependencies essential for reducing uncertainty due to occlusion or depth ambiguity in 3D human pose estimation.
- Designed network architecture that includes flexible graph convolutional layers and a global response normalization layer.

Model Architecture



Method

Flexible Graph Convolutional Network. Central to graph neural networks lies the fundamental concept of the feature propagation rule, which determines how information is transmitted among nodes in a graph. To this end, we propose a flexible graph convolutional network (Flex-GCN) with the following layer-wise update rule for node feature propagation:

$$\mathbf{H}^{(\ell+1)} = \sigma\left(\left((1-s)\mathbf{I} + s\hat{\mathbf{A}}\right)\hat{\mathbf{A}}\mathbf{H}^{(\ell)}\mathbf{W}^{(\ell)} + \mathbf{X}\tilde{\mathbf{W}}^{(\ell)}\right),$$

$$\ell = 0, \dots, L-1$$

where $s \in (0, 1)$ is a positive scaling parameter, $\mathbf{W}^{(\ell)}$ and $\tilde{\mathbf{W}}^{(\ell)}$ are learnable weight matrices, $\sigma(\cdot)$ is an element-wise activation function, $\mathbf{H}^{(\ell)} \in \mathbb{R}^{N \times F_\ell}$ is the input feature matrix of the ℓ -th layer with F_ℓ feature maps. The input of the first layer is $\mathbf{H}^{(0)} = \mathbf{X}$.

Flex-GCN Network Design.

- The input 2D pose undergoes a flexible graph convolutional layer, followed by a GELU activation function.
- Residual block consists of three flexible graph convolutional (Flex-GCNConv) layers.
- In each block, the first two convolutional layers are followed by layer normalization, while the third one is followed by GELU.
- This residual block is repeated four times. Then, a global response normalization (GRN) layer is applied after the residual blocks.
- The last flexible graph convolutional layer of the network generates the 3D pose.

Results

Comparison of our model and baseline methods in terms of MPJPE in millimeters, computed between the ground truth and estimated poses on Human3.6M under Protocol #1.

Method	Dire.	Disc.	Eat	Greet	Phone	Photo	Pose	Purch.	Sit	SitD.	Smoke	Wait	WalkD.	Walk	WalkT.	Avg.
Liu [2]	46.3	52.2	47.3	50.7	55.5	67.1	49.2	<u>46.0</u>	60.4	71.1	51.5	50.1	54.5	40.3	43.7	52.4
Zou [7]	49.0	54.5	52.3	53.6	59.2	71.6	49.6	49.8	66.0	75.5	55.1	53.8	58.5	40.9	45.4	55.6
Xu [4]	47.1	52.8	54.2	54.9	63.8	72.5	51.7	54.3	70.9	85.0	58.7	54.9	59.7	43.8	47.1	58.1
Zou [8]	48.4	53.6	49.6	53.6	57.3	70.6	51.8	50.7	62.8	74.1	54.1	52.6	58.2	41.5	45.0	54.9
Quan [3]	47.0	53.7	50.9	52.4	57.8	71.3	50.2	49.1	63.5	76.3	54.1	51.6	56.5	41.7	45.3	54.8
Zou [9]	45.4	<u>49.2</u>	<u>45.7</u>	<u>49.4</u>	<u>50.4</u>	58.2	47.9	<u>46.0</u>	<u>57.5</u>	<u>63.0</u>	<u>49.7</u>	<u>46.6</u>	52.2	<u>38.9</u>	<u>40.8</u>	<u>49.4</u>
Lee [1]	46.8	51.4	46.7	51.4	52.5	59.7	50.4	48.1	58.0	67.7	51.5	48.6	54.9	40.5	42.2	51.7
Zhang [5]	<u>45.0</u>	50.9	49.0	49.8	52.2	60.9	49.1	46.8	61.2	70.2	51.8	48.6	54.6	39.6	41.2	51.6
Ours	40.2	45.8	45.0	46.8	48.6	<u>54.0</u>	42.4	42.1	53.2	66.7	45.6	45.4	48.8	38.4	40.1	46.9

Comparison of our model and baseline methods in terms of PA-MPJPE, computed between the ground truth and estimated poses on Human3.6M under Protocol #2.

Method	Dire.	Disc.	Eat	Greet	Phone	Photo	Pose	Purch.	Sit	SitD.	Smoke	Wait	WalkD.	Walk	WalkT.	Avg.
Liu [2]	35.9	40.0	38.0	41.5	42.5	51.4	37.8	36.0	48.6	56.6	41.8	38.3	42.7	31.7	36.2	41.2
Zou [7]	38.6	42.8	41.8	43.4	44.6	52.9	37.5	38.6	53.3	60.0	44.4	40.9	46.9	32.2	37.9	43.7
Xu [4]	36.7	39.5	41.5	42.6	46.9	53.5	38.2	36.5	52.1	61.5	45.0	42.7	45.2	35.3	40.2	43.8
Zou [8]	38.4	41.1	40.6	42.8	43.5	51.6	39.5	37.6	49.7	58.1	43.2	39.2	45.2	32.8	38.1	42.8
Quan [3]	36.9	42.1	40.3	42.1	43.7	52.7	37.9	37.7	51.5	60.3	43.9	39.4	45.4	31.9	37.8	42.9
Zou [9]	35.7	38.6	36.3	<u>40.5</u>	39.2	<u>44.5</u>	37.0	35.4	<u>46.4</u>	51.2	<u>40.5</u>	35.6	41.7	30.7	33.9	<u>39.1</u>
Lee [1]	35.7	39.6	37.3	41.4	40.0	44.9	37.6	36.1	46.5	54.1	40.9	36.4	42.8	31.7	34.7	40.3
Zhang [5]	<u>35.3</u>	39.3	38.4	40.8	41.4	45.7	<u>36.9</u>	<u>35.1</u>	48.9	55.2	41.2	36.3	42.6	30.9	33.7	40.1
Ours	34.1	38.0	<u>36.8</u>	39.7	39.2	43.6	33.4	34.5	44.2	57.1	38.3	<u>36.0</u>	<u>41.0</u>	29.9	33.1	38.6

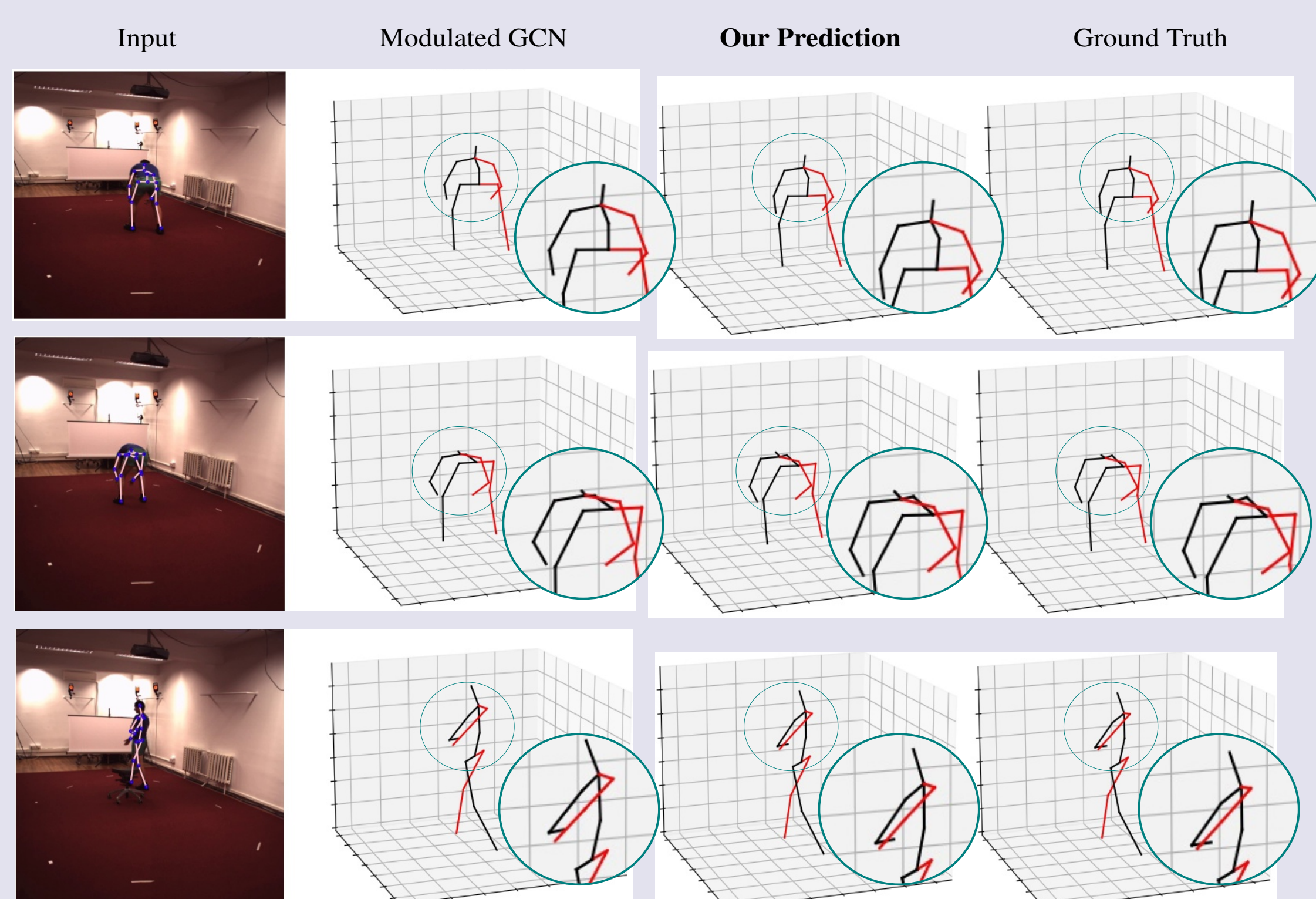


Figure : Visual comparison

Method	PCK (↑)	AUC (↑)
Xu <i>et al.</i> [18]	80.1	45.8
Zeng <i>et al.</i> [20]	<u>82.1</u>	46.2
Lee <i>et al.</i> [4]	81.6	<u>50.3</u>
Zhang <i>et al.</i> [21]	81.1	49.9
Ours	85.2	51.8

Table 3:MPI-INF-3DHP

Results and Ablation study

Performance comparison using the ground truth 2D pose as input.

Method	MPJPE (↓)	PA-MPJPE (↓)
SemGCN [6]	42.14	33.53
High-order GCN [7]	39.52	31.07
Modulated GCN [9]	38.25	30.06
Weight Unsharing [2]	37.83	30.09
Ours	37.41	29.87

Runtime analysis.

Method	Inference Time
High-Order GCN [7]	.013s
Weight Unsharing [2]	.032s
MM-GCN [1]	.009s
Modulated GCN [9]	.010s
Ours	0.06s

Ablation study

Effect of initial residual connection (IRC).

Method	MPJPE (↓)	PA-MPJPE (↓)
Without IRC	39.76	31.25
With IRC	37.41	29.87

symmetry of modulation adjacency.

Method	MPJPE (↓)	PA-MPJPE (↓)
Without Symmetry	37.99	30.11
With Symmetry	37.41	29.87

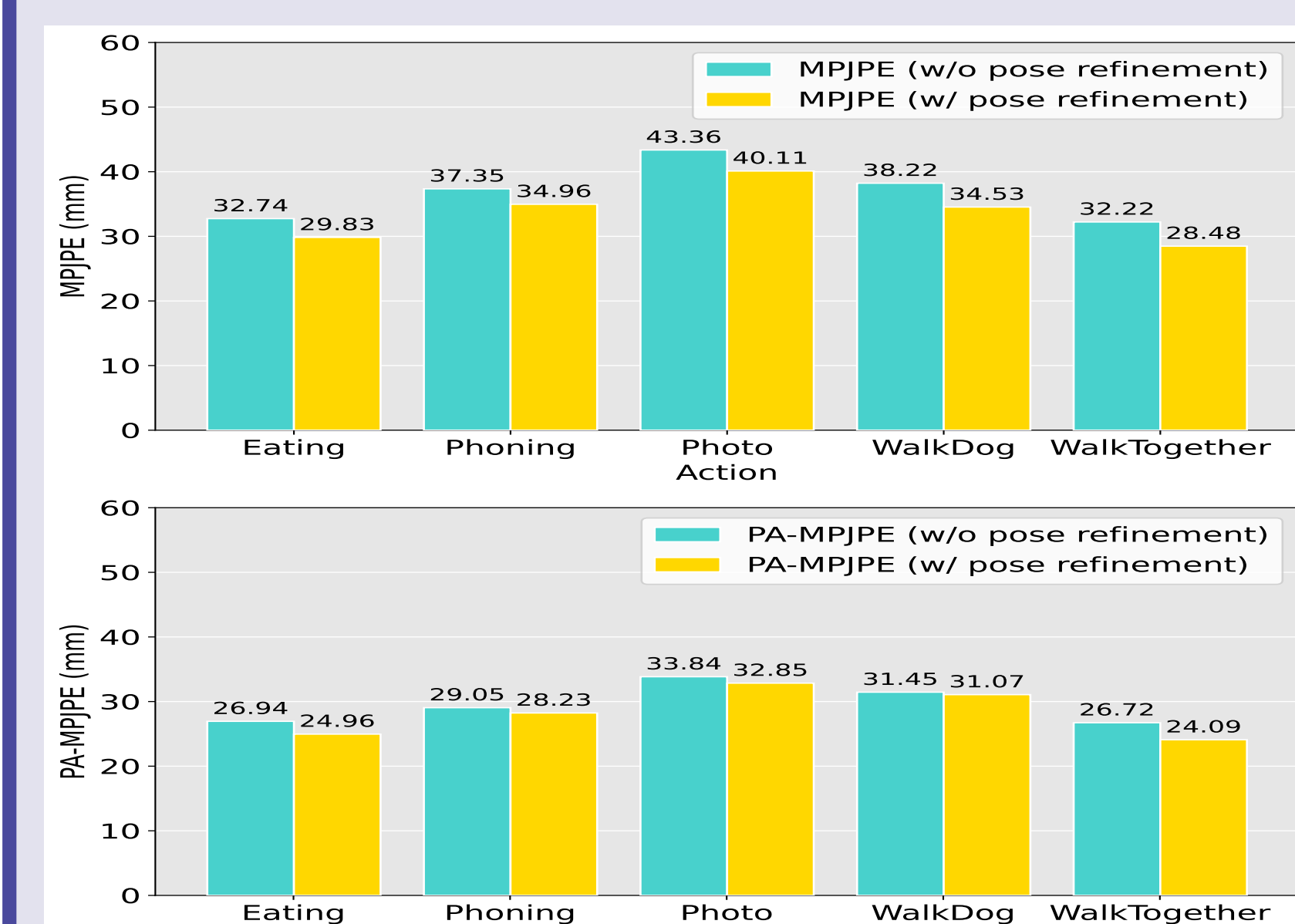


Figure :With and without pose refinement
Note on reproducibility: Code and pre-trained models are available:

<https://github.com/shahjahan0275/Flex-GCN>